

THE EFFECT OF THE SCALP AND THE SKULL BONE IN THE TOTAL IMPEDIVITY OF THE NEONATAL HEAD AND ITS IMPLICATIONS IN THE DETECTION OF BRAIN CELLULAR EDEMA

F. Seoane^{*,**} and K. Lindecrantz^{*}

^{*}School of Engineering, University College of Borås, Borås, Sweden.

^{**}Department of Signal and Systems, Chalmers University of Technology, Gothenburg, Sweden.

fernando.seoane@hb.se

Abstract: Hypoxic-ischemic encephalopathy (HIE) affects severely and frequently on newborns and yet not an efficient detection method has been implemented to assist the early initiation of a saving therapy. Invasive measurements of electrical bioimpedance can be used to detect the changes in the electrical properties of brain tissue as a consequence of the hypoxic cellular edema. In the case of non-invasive measurement the skull and the scalp will modified the measurements in a certain way. In this work, using numerical calculations on a four-concentric spheres model, we study the contribution of the scalp and the skull bone to the total equivalent impedivity, complex resistivity, of the neonatal head and its effect on the non-invasive detection of brain cellular edema. The results confirm the importance of the reactive part of the impedivity on the electrical bioimpedance monitoring of hypoxic brain damage.

Introduction

Perinatal asphyxia, with a high morbidity up to 1.0 - 1.5 % [1] and a extremely high death rate up to 20% mortality in the affected neonates, remains among the most common causes of brain damage and consequent neurological disease in newborns [2] and yet not an efficient monitoring method has been implemented yet.

Founded on the fact that cell swelling, an intrinsic phenomenon to the hypoxic/ischemic injury mechanism, modifies the electrical properties of brain tissue during hypoxia/ischemia, changes on the electrical impedance of tissue have been proposed as a possible indicator of cellular edema. The bases of the potential use of electrical bioimpedance monitoring for early detection of brain damage or even threatening damage in the newborn has been studied since a long time [3,4], especially in the last decades [4-8]. The studies performed to date have reported encouraging results indicating that the alterations in the electrical properties of the brain caused by the hypoxic/ischemic cellular edema can be measured and detected by means of electrical bioimpedance spectroscopy.

All of those successful studies that have performed non-invasive measurements [4,7,9] have reported a highly detrimental impact in the detection of changes in

the brain impedance due to the scalp and the skull bone. The observed changes in the non-invasive case were down to 10 times smaller than in the invasive case. These studies reported data only at one single frequency and the studies were limited also to the dynamics of the resistance, thus ignoring the reactance.

The few works specifically studying the effect of the skull bone and the scalp in the measurements of electrical bioimpedance have been limited again to a single frequency [4,10] once again ignoring the reactance. Therefore there is a lack of available information regarding frequency and as well as reactance.

The high resistivity of the skull bone and the low resistivity of the scalp will affect the distribution of the electrical current flowing through the head differently for different frequencies, thus modifying the measurement scenario as a function of the frequency.

In order to properly evaluate the potential use of electrical bioimpedance spectroscopy for the development of a method for early detection of hypoxic/ischemic brain damage, it is necessary to perform a complete investigation, studying the effect of the scalp and the skull bone in non-invasive measurements of transcephalic electrical impedance.

In this work we investigate the contribution of the scalp and skull bone conductivity to the total impedivity (specific impedance) of the head in the neonate and its implication to detection of changes in the encephalic impedance. The study considers both resistive and reactive components of the impedivity in a broad frequency range.

Methods

Based on a concentric spheres model of the neonatal head following the same approach used by Murray *et al* and Gibson *et al* [4,10], we have performed numerical calculations on two models.

We used a four-layers model (scalp, skull bone, CSF and brain) for the non-invasive case and a two-layers model (CSF and brain) for the invasive case. The concentric spheres building up the models were considered solid, except the innermost. The innermost sphere, brain tissue, was modelled as a suspension of non-deformable spherical cells [11].

Table 1: Resistivity and radius values used in the numerical calculations.

Source	Resistivity (Ωm)	Tissue Element	Radius (cm)	Source
-----	Variable, see Table 2	Brain	4.70	(Murray, 1981)
(Geddes and Baker, 1967)	0.56	C.S.F.	4.80	(Murray, 1981)
(Murray, 1981)	5	Skull	4.93	(Murray, 1981)
(Malmivuo, 1995)	2.2	Scalp	5.25	(Murray, 1981)

Using Mathematica[®] software package, the total specific impedance was calculated following the article 313 in Maxwell's treatise of Electricity & Magnetism [12] For each of the models the impedivity was calculated for increasing values of the radius of the suspended cells, simulating the effect of brain cell swelling. The maximum volume factor obtained increasing the radius was $0.7404 \approx \pi/\sqrt{18}$, maximum packing of non-deformable spheres according to the Kepler conjecture and hales proof [13].

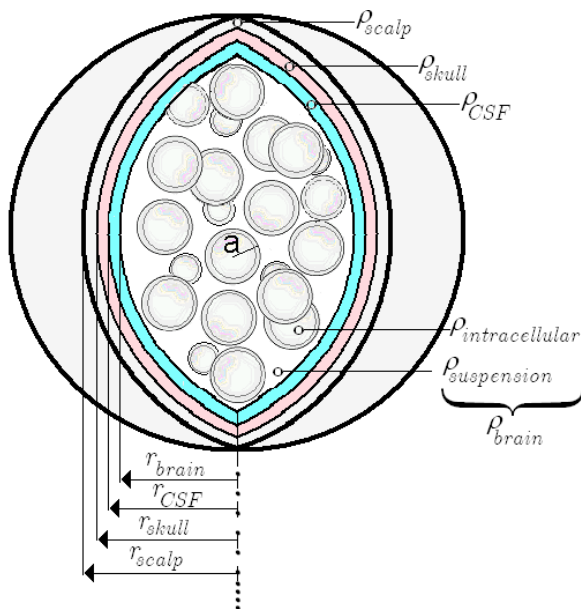


Figure 1: 4-concentric sphere model used in the numerical calculations

The radius value used for each of the concentric sphere is the same as in Murray's model [4], except for the innermost sphere modelling the cerebral ventricles, not applicable in this study. The spheres modelling the scalp, skull and the CSF layer were considered isotropic and the resistivity values used in the calculations have been selected from different literature sources [4,14,15], according to Table 1. The resistivity values used for the suspension of cells are 1.1 and 3.3 Ωm for intra- and extracellular fluid respectively, both values from [15]. See Table 2.

Table 2: Resistivity and radius values used in the brain model as a suspension of cells.

Brain Element	Radius (μm)	Resistivity (Ωm)	Resistivity Source
Intracellular fluid	10 – 10.7265	1.1	(Malmivuo, 1995)
Suspension fluid	47×10^3	3.3	(Malmivuo, 1995)

The obtained impedivity is a complex number composed by the specific resistance, real part, and the specific reactance, imaginary part. It is also denominated complex resistivity and it is denoted by ρ . See equation (1).

$$\rho = \rho' - j\rho'' \quad (1)$$

Results

In figure 2, the resulting specific impedance, from both cases, is plotted in the complex plane for two different radii of the suspended spherical cells. In the obtained Wessel plot it is easy to observe the effect of the scalp and skull bone in measurement scenario.

For a normal cell radius, no cell swelling present, we observe a significant clear difference in both real and imaginary parts of the impedivity between the invasive and the non-invasive case. The effects are easier to notice at low frequencies and the reactive part changes in a different way that the resistive part. In the non-invasive case, the reactive part is smaller at any frequency, while the resistivity is smaller at lower and larger at higher frequencies. Also the frequency dependency of the specific impedance changes; the characteristic frequency, *frequency at the maximum reactive part*, increases from 260 kHz in the invasive case to 380kHz in the non-invasive case.

In Figure 2 it is also possible to notice a certain influence of the scalp and the skull bone in the changes of impedivity as a consequence of swelling of the cells in suspension inside the innermost sphere. We can appreciate that those changes are affected, both in absolute and relative terms.

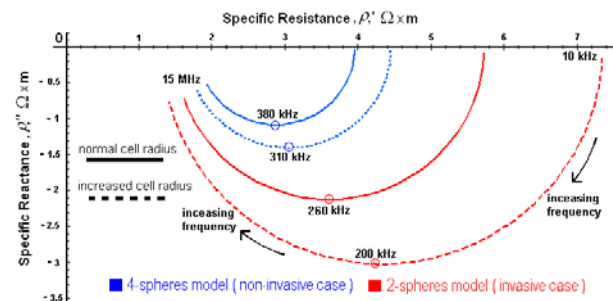


Figure 2: Wessel plot in the complex plane of the impedivity of the equivalent spheres for both cases.

The mentioned influence can be more accurately examined in Figures 3 and 4, where the impedivity, obtained from each of the cases, is decomposed in its resistive and reactive parts. The calculated variation in

each component is independently plotted for both cases and compared in terms of variation over the baseline versus frequency. The specific resistance is plotted in Figure 3 and the data regarding the reactive component is plotted in Figure 4.

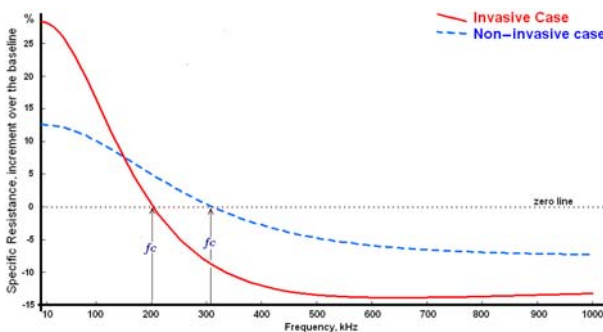


Figure 3: Variation of the specific resistance during cell swelling for both, invasive and non-invasive cases.

In Figure 3 we can observe that the changes in the specific resistance during cell swelling are attenuated by the influence of the scalp and skull at almost any frequency, with the exception of a frequency window around the characteristic frequency of the invasive case, 200 kHz. The highest attenuation is produced in the same frequency range. An interesting result that can be seen in this plot is that the zero-crossing point, *i.e.* when the increment becomes a decrement, occurs at the characteristic frequency in both cases.

In the case of the specific reactance we can observe in Figure 4 a high attenuation in the calculated increment at low frequencies and a slight growth at high frequencies. We can also notice that the turning point from attenuation to growth occurs at the characteristic frequency of the normal invasive case, no swelling.

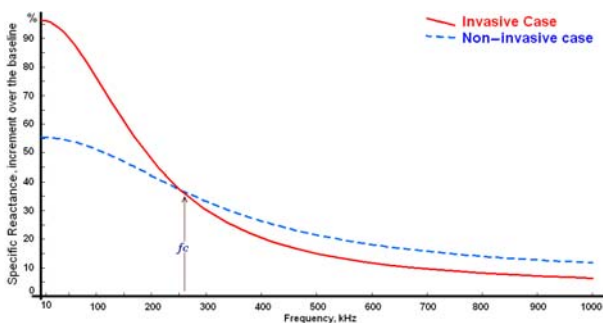


Figure 4: Variation of the specific reactance during cell swelling for both, invasive and non-invasive cases.

Discussion

As expected, due to the skull bone and the scalp the measurement scenario between the invasive case and the non-invasive case does differ affecting both the resistive and the reactive part of the total specific impedance. The observed effect affects the specific resistance and reactance in different manners, exhibiting certain frequency dependency.

In this respect, the resistivity is affected the most at low and high frequencies while at medium frequencies the changes are small, approaching the characteristic frequency, or none at the characteristic frequency. So the resistivity changes the most, precisely when the resistive character is the predominant in specific impedance of tissue, *i.e.* small phase angle. In the case of the specific reactance, it is notably affected at any frequency especially at low frequencies.

In the case of resistivity the larger changes occur, both proportionally and absolutely, at low frequencies while in the case of the specific reactance, proportionally, it changes the most at low frequencies but in magnitude the largest change is exhibited at medium frequencies, when the reactive character is predominant over the resistive.

In terms of variation of the total impedance as a consequence on internal cell swelling, the scalp and skull bone affect both real and the imaginary parts and again an expected frequency dependency is exhibited.

In the case of the real part, the changes are attenuated at low frequencies, in concordance with previous reported studies [5,16], as well as at high frequencies. However there is a frequency window where the changes are enlarged instead of weakened at medium frequencies, around the characteristic frequency.

In the case of the reactive part, the resulting attenuation occurs only below the characteristic frequency in the manner that the lower the frequency the higher the attenuation. At higher frequencies the changes were affected in minor manner, exhibiting an enlargement instead of attenuation.

Conclusion

It is encouraging to observe that in the detection of changes in the electrical properties of tissue as a consequence of cells swelling, the effect of the skull bone and the scalp on the total specific impedance is not negative at all frequencies, and when negative at least not destructive.

The calculated skull and scalp effect on the specific reactance enlarging the changes due to internal cell swelling strengthens the importance of the reactance for the monitoring of changes in the brain electrical impedance as a consequence of hypoxia/ischemia.

Acknowledgements

We would like to acknowledge the financial support of the Swedish Research Council (research grant number 2002-5487) and the European Commission (The BIOPATTERN Project, Contract No. 508803).

References

- [1] LEGIDO, A., KATSETOS, C.D., MISHRA, OP., and DELIVORIA-PAPADOPOULOS, M. (2000): 'Perinatal Hypoxic Ischemic Encephalopathy: Current and Future Treatments', *International Pediatrics*, **15**, pp. 143-151

- [2] VANNUCCI, RC., and PERLMAN, JM. (1997): 'Interventions for Perinatal Hypoxic-Ischemic Encephalopathy', *Pediatrics*, **100**, pp. 1004-1014
- [3] VAN HARREVELD, A. (1957): 'Changes in Volume of Cortical Neuronal Elements during Asphyxiation', *Am J Physiol.*, **191**, pp. 233-242
- [4] MURRAY, PW. (1981): 'Field Calculations in the Head of a Newborn Infant and Their Application to The Interpretation of Transephalic Impedance Measurements', *Med. Biol. Eng. Comput.*, **19**, pp. 538-546
- [5] WILLIAMS, CE., GUNN, A., GLUCKMAN, PD. (1991): 'Time Course of Intracellular Edema and Epileptiform Activity Following Prenatal Cerebral Ischemia in Sheep', *Stroke*, **22**, pp 516-521
- [6] HOLDER, DS. (1992): 'Detection of Cerebral Ischaemia in the Anaesthetised Rat by Impedance Measurement with Scalp Electrodes: Implications for Non-Invasive Imaging Of Stroke by Electrical Impedance Tomography', *Clinical Physics and Physiological Measurement*, **13**, pp. 63-75
- [7] LINGWOOD, BE., DUNSTER, KR., COLDITZ, PB., and WARD, LC. (2002): 'Noninvasive Measurement of Cerebral Bioimpedance for Detection of Cerebral Edema in the Neonatal Piglet', *Brain Research*, **945**, pp. 97-105
- [8] SEOANE, F., LINDECRANTZ, K., OLSSON, T., KJELLMER, I., FLISBERG A., and BAGENHOLM, R. (2005): 'Spectroscopy Study of the Dynamics of the Transencephalic Electrical Impedance in the Perinatal Brain during Hypoxia', *Physiological Measurement*, **26**, pp. 849-863
- [9] HOLDER, DS. (1992): 'Detection Of Cortical Spreading Depression in The Anaesthetised Rat By Impedance Measurement with Scalp Electrodes: Implications for Non-Invasive Imaging of the Brain with Electrical Impedance Tomography', *Clinical Physics and Physiological Measurement*, **22**, pp. 77-86
- [10] GIBSON, A., BAYFORD, RH., and HOLDER, DS. (2000): 'Two-Dimensional Finite Element Modelling of the Neonatal Head', *Physiological Measurement*, **21**, (1): 45-52
- [11] COLE, KS. (1928): 'Electric Impedance of Suspensions of Spheres', *Journal of General Physiology*, **12**, pp. 29-36
- [12] MAXWELL, JC. (1891): 'A Treatise on Electricity & Magnetism', (Clarendon Press, Oxford).
- [13] HALES, T. (2004): 'Formalizing the Proof of the Kepler Conjecture' Proc. of Theorem Proving in Higher Order Logics. 17th International Conference, TPHOLs 2004, Park City, UT, USA, pp. 305-320
- [14] GEDDES, LA., and BAKER, LE. (1967): 'The Specific Resistance of Biological Material - A Compendium of Data for the Biomedical Engineer and Physiologist', *Med. Biol. Eng.*, **5**, pp. 271-293
- [15] MALMIVUO, J., and PLONSEY, R. (1995): 'Bioelectromagnetism - Principles and Applications of Bioelectric and Biomagnetic Fields', (Oxford University Press, New York).
- [16] LINGWOOD, BE., DUNSTER, KR., HEALY, GN., WARD, LC., and COLDITZ, PB. (2003): 'Cerebral Impedance and Neurological Outcome Following a Mild or Severe Hypoxic/Ischemic Episode in Neonatal Piglets', *Brain Research*, **969**, pp. 160-716